Residual Demand Modeling and Application to Electricity Pricing

Andreas Wagner*

Fraunhofer ITWM
Department for Financial Mathematics
Fraunhofer-Platz 1
67663 Kaiserslautern
Germany
andreas.wagner@itwm.fraunhofer.de

Abstract

A model for residual demand is proposed, which extends structural electricity price models to account for renewable infeed in the market. Infeed from wind and solar is modelled explicitly and withdrawn from total demand. The methodology separates the impact of weather and capacity. Efficiency is modelled as a stochastic process. Installed capacity is a deterministic function of time. The residual demand model is applied to the German day-ahead market. Price trajectories show typical features seen in market prices in recent years. The model is able to closely reproduce the structure and magnitude of market prices. Using simulations it is found that renewable infeed increases the volatility of forward prices in times of low demand, but can reduce volatility in peak hours. The merit-order effect of increased wind and solar capacity is calculated. It is found that under current capacity levels in the German market wind has a stronger overall effect than solar, but both are even in peak hours.

Keywords: residual demand modeling, electricity pricing, renewable infeed, wind infeed, solar infeed, electricity demand, German power market, merit-order effect, structural model

*The author is grateful for the financial support received from the Innovation Center Applied System Modeling. Moreover, the author thanks the anonymous referees for their f

1 Introduction

Electricity price models, which use demand as a state variable are known as *structural*, *hybrid* or *supply/demand* models. In this class of models, the supply side (electricity production) and the demand side (electricity consumption) are described separately[1]. The market price of electricity is determined by the marginal production unit in the merit order. All models in the literature use demand as a state variable, which is the only one in the early work by Barlow (2002). More recent approaches further include capacity (cf. Cartea and Villaplana, 2008), fuel prices (cf. Pirrong and Jermakyan, 2008; Coulon and Howison, 2009; Smeers and de Maere, 2010; Carmona et al., 2011)[2], or both (cf. Aïd et al., 2009, 2012). Lyle and Elliott (2009) and Burger et al. (2004) also have a load dependent component in their model. Demand therefore plays a key role in those models and should be modelled carefully. A survey on this class of models including its benefits and obstacles as well as some extensions is given in Carmona and Coulon (2012).

In recent years there has been a rapid growth in installed capacity of renewable energy sources (hydro, wind, solar[3], biomass, geothermal), which is expected to continue for decades. Half of the worldwide newly added capacity in 2010 has been of renewable technologies (including hydro). In the European Union, renewables account for more than 40% of yearly capacity additions since 2005[4]. Due to strong political support, especially Germany already has a considerable high share of wind and solar power plants in its electricity system. By September 2012, Germany had 29 GW installed capacity of wind power plants and 30 GW installed capacity of solar power plants, which together accounts for about 35% of total installed capacity[5]. In 2011, 20% of German electricity consumption has been produced by renewable sources[6]. Scenarios[7] for the year 2022 see renewable installed capacity in Germany between 93 GW and 150 GW, which is (much) more than the German yearly peak demand (in 2010 at about 83 GW). In all those scenarios, conventional installed capacity is predicted to decrease to between 82 GW and 92 GW.

This considerable amount of renewables sources in the system and the regulatory circumstances (see below) heavily influence the electricity price for Germany, which is traded at the EEX and EPEX. In figure 1 an hourly production stack and the corresponding market prices are displayed. Supply is split in production from wind, production from solar and residual production, which is covered by technologies other than wind and solar, i.e. mainly conventional generation units like nuclear, lignite, coal, and gas. The prices follow the profile of residual production, so we conclude that the intra-day price shape heavily depends on the amount

[1] Therefore we favor the term *supply/demand models* and use it throughout this work.
[2] Pirrong and Jermakyan (2008) and Smeers and de Maere (2010) use a reflected load process in order to capture capacity constraints.
[3] In this paper we use the term *solar* for electricity production from solar energy. This technique is known as *photovoltaics*.
[4] Figures available until 2010, Renewable Energy Policy Network for the 21st Century (2011).
[5] Own calculations based on data from `http://www.bundesnetzagentur.de`.
[6] Bundesministerium für Umwelt Naturschutz und Reaktorsicherheit (2012)
[7] 50hertz et al. (2011)

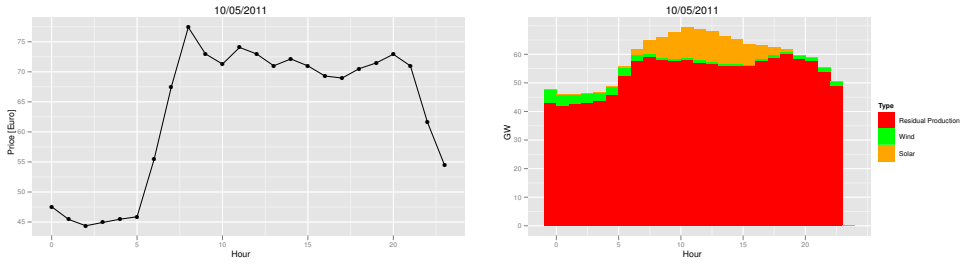

Figure 1: EPEX spot market prices and production profiles for Germany on a day with high renewable infeed.

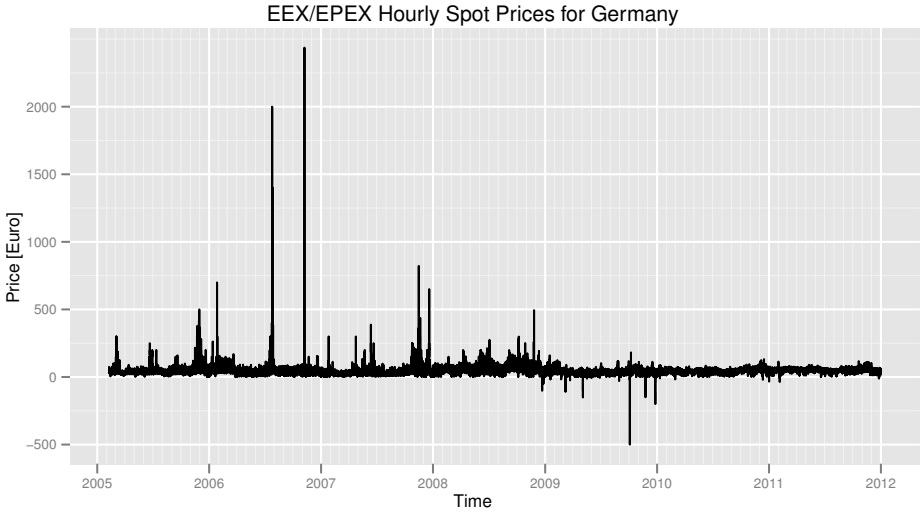

Figure 2: EEX/EPEX hourly spot prices from the year 2005 through 2011.

of renewable infeed

In this paper we suggest a model which extends existing models in this direction, as this is not accounted for in existing supply/demand models in the literature. Moreover, the model components can be used in economic models for the generation of wind and solar production time-series[8].

The effect of renewable infeed is also seen in time-series of hourly spot prices as plotted in figure 2 from 2005 to 2011. There are less positive spikes since 2009 and they also reduced in magnitude. On the other hand, negative prices started to occur and especially in 2009 negative spikes are much more present than positive ones. In 2010 and 2011, the size of negative spikes reduced, indicating that producers are learning and trying to avoid negative prices (e.g. by assembling a more flexible power plant portfolio). The time series for 2011 in figure 3 reveals that there are still some moderate spikes in the market, both positive and negative. The typical situation in case of negative spikes is a very high renewable infeed (usually for

[8]Usually historical profiles are used, but especially in scenario-analysis the limited historical data is not sufficient.

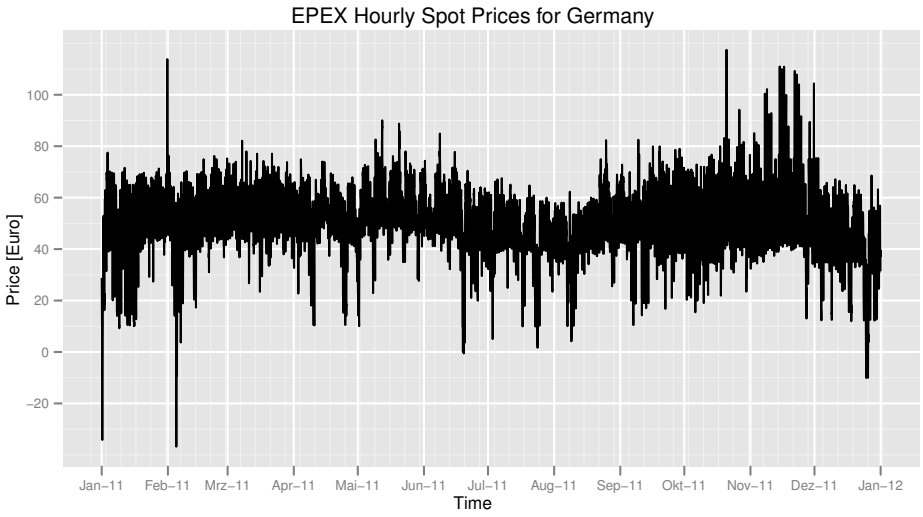

Figure 3: EPEX hourly spot prices for the year 2011.

a few hours only, caused by fluctuating wind infeed) on days with generally low demand (public holiday, weekend). The electricity oversupply during those hours is caused by baseload plants, which cannot be economically switched off for a few hours only (there are also technical restrictions). They are prepared to accept negative prices for a short time period in order to be able to continue with their production. Positive spikes occur usually in times of high conventional demand. Germany has enough conventional capacity to meet peak demand even in times of zero renewable infeed (Bundesnetzagentur, 2011b), but the conventional capacity is near its limit in those situations. Further causes of positive spikes are unexpected outages. The increasing share of solar infeed is reducing the (positive) spike risk. Solar produces mainly during hours of peak demand, so it reduces conventional peakload. This is the *peak-shaving effect*, which is also visible since 2010 in figure 1. A third characteristic of spot-prices seen in the figures is the seasonality on different time-scales. There is intra-day seasonality (figure 1), weekly seasonality (figure 3) and a yearly seasonality (figure 3 and 2).

Production from renewables introduces new uncertainty (=risk) to the market due to their volatile production profile. Therefore in order to apply supply/demand models on the German power market (or any other market with a high share of renewables in its system), the infeed from wind and solar power plants should be considered, especially as the seasonalities in electricity prices are mainly generated by the seasonalities in residual production. As supply and demand must coincide at every time we use *residual demand* in the following, as we include the renewables on the demand side of the model.

The main contributions of this work are explicit models for wind and solar power infeed, which are used to

refine existing supply/demand models for electricity. Moreover, within a simple structural framework, the residual demand model is applied to the German market. Our empirical work is also based on the German power market.

The regulatory circumstances in Germany are based on the EEG[9]. It implies that all production from renewables must be fed into the electricity grid. Conventional generation units (nuclear, lignite, hard coal, gas, oil, pumped storage) are to cover the residual demand only. As an incentive to investors, a guaranteed tariff for the produced electricity is paid for 20 years after the installation of the plant (*feed-in tariff*). We will model wind and solar only, as they have a particularly uncertain and fluctuating infeed profile (unlike hydro or biomass). As most of the wind and solar power plants have been built in recent years they are eligible for the feed-in tariff and infeed priority and bid as must-run in the day ahead auction (basically they bid at the lowest price allowed). Therefore we can consider the production from renewables as a demand reduction, i.e.

$$\text{residual demand} = \text{(stochastic) total demand} - \text{(stochastic) infeed from renewables.} \tag{1}$$

Residual (or conventional) demand is the electricity to be generated by conventional technologies. This is the demand which should be used in the merit order of conventional generation units to determine the market price.

A common approach in demand modeling in the literature (i.e. the supply/demand models cited above) is to choose a deterministic seasonal component plus a stochastic process modeling random deviations from the seasonal level. They occur mainly due to weather conditions, i.e. an unusual cold spell in spring will cause a rise in demand for a few days due to electric heating. As those deviations are temporary only the stochastic process is mean-reverting to level zero. Any trend or seasonality is contained in the deterministic component. As an example we introduce a model for total system load with the desired properties using an Ornstein-Uhlenbeck process, which is used in Aïd et al. (2009), Coulon and Howison (2009), and Lyle and Elliott (2009). We measure time continuously in years and denote it by $t \in [0, T]$, where $T > 0$ is some finite time horizon. All processes are defined on a probability space $(\Omega, \mathbb{P}, \mathcal{F})$ supporting Brownian motion with the filtration $\{\mathcal{F}_t\} = \{\mathcal{F}_t\}_{t\in[0,T]}$ generated by all the Brownian motions W_t used in this paper.

Model 1.1 (Model for total system load)**.** *Denote total system load at time $t \in [0, T]$ by L_t and assume*

$$L_t = \psi_t + l_t, \tag{2}$$

[9] EEG is short for *Erneuerbare-Energien-Gesetz* (Renewable Energy Sources Act), see `http://www.erneuerbare-energien.de` for more information such as laws, statistics, etc.

where

ψ_t *is a time-dependent deterministic load forecast, and*

l_t *is an Ornstein-Uhlenbeck process with mean-reversion speed* $\theta^{\text{load}} > 0$ *and volatility* $\sigma^{\text{load}} > 0$*, i.e.*

$$dl_t = -\theta^{\text{load}} l_t \, dt + \sigma^{\text{load}} \, dW_t^{\text{load}}, \quad l_0^{\text{load}} = l_0. \tag{3}$$

Model 1.1 is formulated in a rather general matter. It can also be applied to log-system load[10] to ensure that total system load is always positive (Coulon and Howison, 2009; Smeers and de Maere, 2010). However, as the size of the seasonal component usually overweighs the stochastic fluctuations by far, the probability of negative values is negligible. An extension with time-dependent parameters is possible (e.g. seasonal volatility as in Cartea and Villaplana, 2008). It is important to note that demand is assumed to be price inelastic, i.e. L_t depends not on the price for electricity. This assumption is common in the literature on supply/demand models. This is obviously a simplification, as in particular market coupling and the trade over interconnectors leads to part of demand to be price sensitive. However, this amount is so far considered negligible, but we expect it to become more important in the future. Nevertheless market coupling is not in the scope this work, so we assume price-inelastic demand in the following.

The intra-day load pattern is very strong and possible deviations from the seasonal mean are usually present all day. Therefore in practice model 1.1 is evaluated once for each day only and the intra-day load curve is derived deterministically from this evaluation. This approach is taken in Smeers and de Maere (2010) and also in section 6 of this work. Aïd et al. (2009) and Coulon and Howison (2009) apply their models only to a single hour of the day and therefore there is no need for intra-day demand in their case studies. When applied to markets with renewables, the demand models are calibrated on total demand minus infeed from renewables. In contrast to the approach taken in this paper such a model does not distinguish between the risk from demand shocks and the uncertainty in renewable infeed. Moreover, it cannot account for the effect of increasing installed renewable capacity and the stochastic change of the intra-day demand profile. Those drawbacks are overcome with the residual demand model proposed in the following.

The remainder of this paper is structured as follows. In section 2 we introduce our approach separating infeed from installed capacity. We apply this to wind and solar power infeed. The model for wind power infeed is introduced in section 3, the model for solar power infeed in section 4. We combine both to construct a model for residual demand in section 5, which we use in a case study on the German market in section 6. Concluding remarks are in section 7.

[10] When modeling log-load, the OU-process in equ. (3) usually has a non-zero mean-reversion level, i.e. it reads $dl_t = \theta^{\text{load}}(\mu^{\text{load}} - l_t) \, dt + \sigma^{\text{load}} \, dW_t^{\text{load}}$.

2 General modeling approach

Installed capacity causes a trend in renewable infeed which has to be accounted for. We model the infeed from renewables independent of the installed capacity by using *efficiency* (also known as *load factor* or *utilization rate*) rather than absolute infeed. With this approach we remove the trend in infeed data caused by changes in installed capacity. In the following, we use the placeholder *src* for the renewable energy source, i.e. wind or solar.

Definition 2.1 (Efficiency)**.** We define the *efficiency* E_t^{src} of the energy source *src* at time t by

$$E_t^{src} = \frac{AI_t^{src}}{IC_t^{src}}, \tag{4}$$

where

$IC_t^{src} > 0$ denotes installed capacity, and

$AI_t^{src} \in [0, IC_t^{src}]$ denotes absolute infeed

of the energy source *src* at time t. By construction we have $E_t^{src} \in [0, 1]$.

In order to extend the range of possible models for E_t we map efficiency on the real line. We use the *logit*-transformation as we found it transforms the data approximately to a normal distribution.

Definition 2.2 (Logit-transformation)**.** The *logit transformation*

$$\text{logit} : (0, 1) \to \mathbb{R} \tag{5}$$

of a variable $x \in (0, 1)$ is defined as (Fahrmeir and Tutz, 2001)

$$\text{logit}(x) = \log\left(\frac{x}{1-x}\right). \tag{6}$$

Due to the open interval of allowed values in the transformation, we must assume that we have neither zero efficiency (i.e. no infeed at all) nor full efficiency (i.e. all installed plants are fully utilized). In later sections we find that this assumption is always fulfilled in our dataset. In the following we look at a random variable, whose logit-transformation is normally distributed.

Definition 2.3 (Logit-normal distribution)**.** Assume a random variable $X \in (0, 1)$ and denote its logit-transformation

$$Y := \text{logit}(X). \tag{7}$$

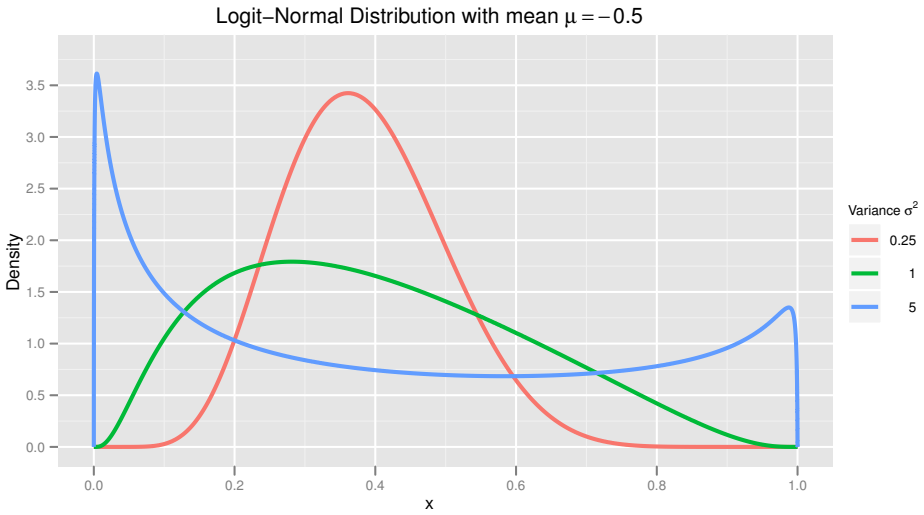

Figure 4: The logit-normal density with different parameters.

Suppose Y is normally distributed with expectation μ and standard deviation σ, i.e.

$$Y \sim N\left(\mu, \sigma^2\right). \tag{8}$$

We call X *logitnormally distributed with mean* μ *and variance* σ^2 and write $X \sim \text{logit}\, N\left(\mu, \sigma^2\right)$.

In figure 4 we plot the logitnormal distribution for different parameter sets. The logit-normal distribution has not found much attention in the literature. It is discussed in an early work by Johnson (1949) and there is recent work of Frederic and Lad (2008). A generalized logitnormal-distribution is analyzed in Mead (1965). Johnson (1949) shows that the density f_X of a logit-normally distributed random variable X is unimodal if

$$\sigma < \sqrt{2}. \tag{9}$$

We do not expect our distribution to be bimodal, as this reflects either very high infeed or rather low infeed. This is a realistic scenario in neither wind nor solar power infeed. Therefore we use equ. (9) to check calibration results.

Remark 2.4 (Parameter estimation for a logitnormally distributed random variable). Given a set of logit-normally distributed observations $A = \{x_1, x_2, \ldots, x_n\}$ the parameters of the logitnormal distribution are estimated in a two-step procedure:

(1) Apply the logit-transformation to the observations, i.e. calculate $\bar{A} = \{\text{logit}(x_i), i = 1, 2, \ldots, n\}$.

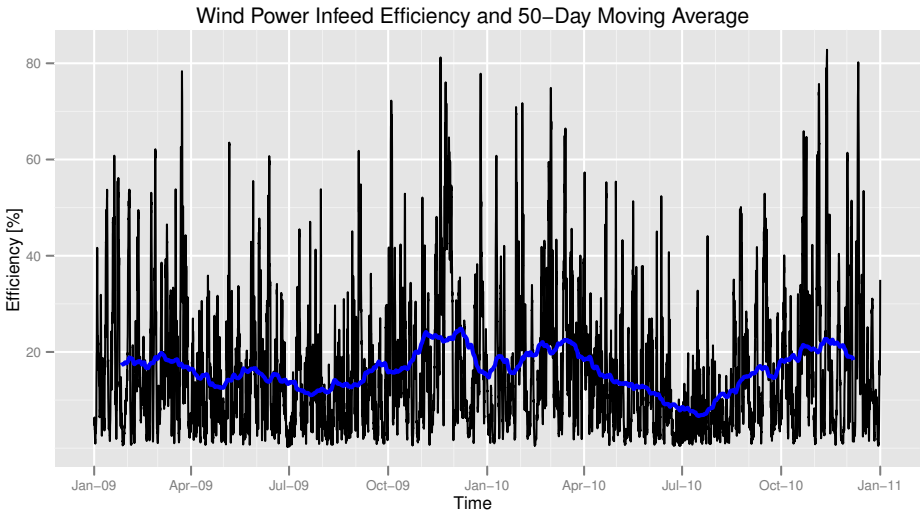

Figure 5: Hourly data of wind power infeed efficiency for Germany in 2009 and 2010, and a centered 50-day moving average.

(2) Use standard methods for the fitting of the normal distribution to $\bar{A}$ like the method of moments or maximum likelihood estimation to obtain the estimated parameters $\hat{\mu}, \hat{\sigma}^2$.

We denote the logit-transformed efficiency

$$\tilde{E}_t^{src} = \text{logit}(E_t^{src}), \tag{10}$$

where $\tilde{E}_t^{src} \in \mathbb{R}$. It splits into a deterministic seasonality $\eta_t^{src} \in \mathbb{R}$ and a (random) deseasonalized efficiency $\bar{E}_t^{src} \in \mathbb{R}$, i.e.

$$\tilde{E}_t^{src} = \eta_t^{scr} + \bar{E}_t^{src} \; \forall \; t \in [0, T]. \tag{11}$$

We assume a yearly seasonality η_t^{scr}, so it must satisfy the condition

$$\eta_t^{scr} = \eta_{t-1}^{scr} \quad \forall \; t \geq 1, \tag{12}$$

in particular this means that η_t^{scr} contains no trend.

3 Model for wind power infeed

There is literature on wind speed models and a good overview on the various distributions proposed is in Carta et al. (2009). Their results indicate that the Weibull distribution is the preferred choice in wind speed mod-

Statistic	No Transformation	Logit	Deseasonalized Logit
mean	0.164	-2.008	0.000
median	0.121	-1.980	0.031
standard deviation	0.143	1.144	1.123
skewness	1.512	-0.045	-0.106
kurtosis	5.394	2.854	2.828
minimum	0.003	-5.770	-3.627
maximum	0.828	1.572	3.366

Table 1: Statistical figures for the wind power efficiency data without transformation, with a logit transformation, and after deseasonalization.

eling. There is also literature on the generation of wind speed time series, i.e. Aksoy (2004) with an overview of the different techniques proposed. Wind is transformed to power in an WECS (wind energy conversion system). The power generated depends on the current wind speed and the power curve of the WECS. As illustrated in Carta et al. (2009), the power curve is a non-linear function of wind speed and air density[11]. Therefore we cannot conclude that wind infeed also follows a Weibull distribution.

To our knowledge, the wind power infeed of a whole country has not yet been described in the literature. We propose a model and motivate our choice with data on actual wind power infeed in Germany from 01/01/2009 to 31/07/2011[12]. Instead of modeling wind speeds and converting it using a power curve we model wind power infeed directly.

In figure 5 we plot the data in terms of efficiency[13] and include a 50-day moving average, which motivates a seasonality with lower infeed in summer compared to the rest of the year. The graph shows strong mean reversion and spikes, i.e. upward jumps followed by a downward jump shortly after. In table 1 we give some statistical figures of the data.

Figure 6 shows wind power infeed efficiency data after a logit-transformation. To account for seasonality we fit a function of the form

$$\eta_t^{\text{wind}} = a\cos(2\pi t + b) + c \tag{13}$$

to the data. This function fulfills the condition in equ. (12). The estimated seasonality is also plotted in figure 6.

In the following we argue for a model describing deseasonalized efficiency $\bar{E}_t^{\text{wind}}$. The histogram of the

[11] The dependence of the power curve on air density is usually neglected in the literature and very often not even published by the manufacturer (Carta et al., 2008).

[12] Data for 2009 has been taken from the four TSOs' websites (`http://www.tennettso.de`, `http://www.50hertz-transmission.net`, `http://www.amprion.net`, and `http://www.enbw.com`) in October 2010. Data for 2010 and 2011 is provided by European Energy Exchange AG (2012). This data is also generated by the TSOs, but compiled into one file for each hour by the EEX.

[13] For 2009, we assume an installed capacity of 25.777 GW (Bundesministerium für Umwelt Naturschutz und Reaktorsicherheit, 2010), for 2010 and 2011 we have 25.961 GW and 27.547 GW, respectively (European Energy Exchange AG, 2012).

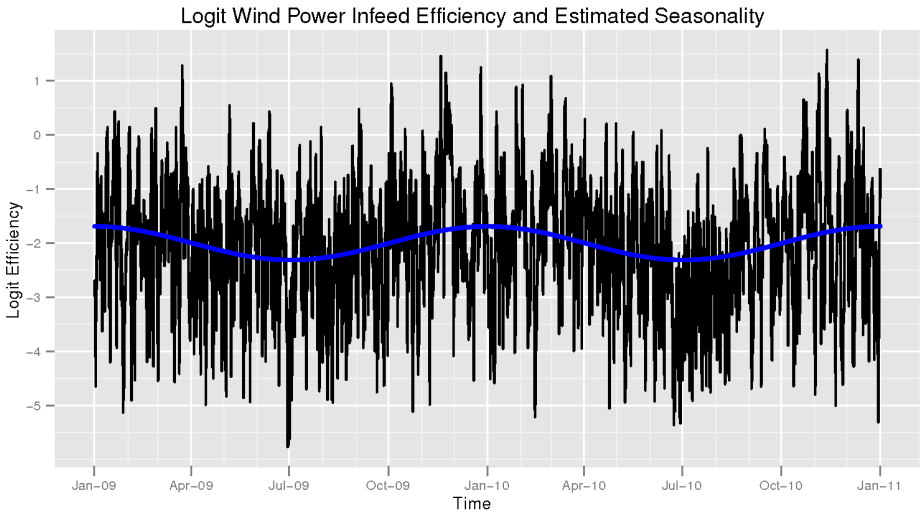

Figure 6: Logit wind power infeed efficiency for Germany in 2009 and 2010, and the seasonality estimate (blue).

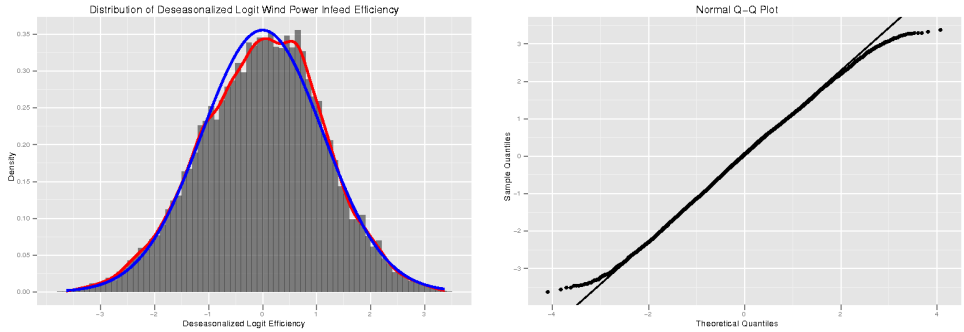

Figure 7: Distribution of deseasonalized logit wind power infeed efficiency. The left plot includes the histogram, empirical distribution (red line), and a fitted normal distribution (blue line), the right plot is the quantile-quantile plot against the normal distribution.

deseasonalized data in figure 7 shows that the empirical distribution of the transformed data is very close to normal. This is also supported by the statistical figures in table 1, which show a skewness close to zero and a kurtosis close to three for the deseasonalized data. Mean and median are close, which points torwards a symmetric distribution such as normal distribution. Further support for the normality assumption is given by a quantile-quantile-plot (also in figure 7), which shows slight deviations from the normality assumption in the tails of the data only. As we aim for a model of wind infeed over time, the results above suggest to model deseasonalized logit wind power efficiency as an Ornstein-Uhlenbeck process, which is stationary normally distributed.

Model 3.1 (Model for wind power efficiency)**.** *The model for deseasonalized logit wind power efficiency* $\bar{E}_t^{\text{wind}}$ *is*

$$d\bar{E}_t^{\text{wind}} = -\theta^{\text{wind}}\bar{E}_t^{\text{wind}}\ dt + \sigma^{\text{wind}}\ dW_t^{\text{wind}}, \quad \bar{E}_0^{\text{wind}} = e_0, \tag{14}$$

where

- e_0 *is the initial value,*
- θ^{wind} *is the mean reversion speed, and*
- σ^{wind} *is the volatility.*

The Ornstein-Uhlenbeck process also fits an autocorrelation. The partial autocorrelation function shows clear autocorrelation in the dataset, which is 0.990 at lag one. There is also significant partial autocorrelation at lag two and three, which the Ornstein-Uhlenbeck process cannot capture. We conclude that it is important to incorporate autocorrelation in the model and that an autoregressive time-series model with higher order (e.g. three) could also be considered as an alternative. As we aim for a continuous model, we focus on model 3.1 in the following.

Proposition 3.2 (Strong solution of $\bar{E}_t^{\text{wind}}$)**.** *The SDE in equ.* (14) *has the strong solution*

$$\bar{E}_t = e_0 e^{-\theta t} + \sigma \int_0^t e^{-\theta(t-s)} dW_s, \tag{15}$$

where we omit the superscript wind *in the parameters for readability.*

Its first two moments are

$$\mathbb{E}\left[\bar{E}_t | \bar{E}_0 = e_0\right] = e_0 e^{-\theta t}, \tag{16}$$

$$\text{Var}\left[\bar{E}_t\right] = \frac{\sigma^2}{2\theta}(1 - e^{-2\theta t}), \tag{17}$$

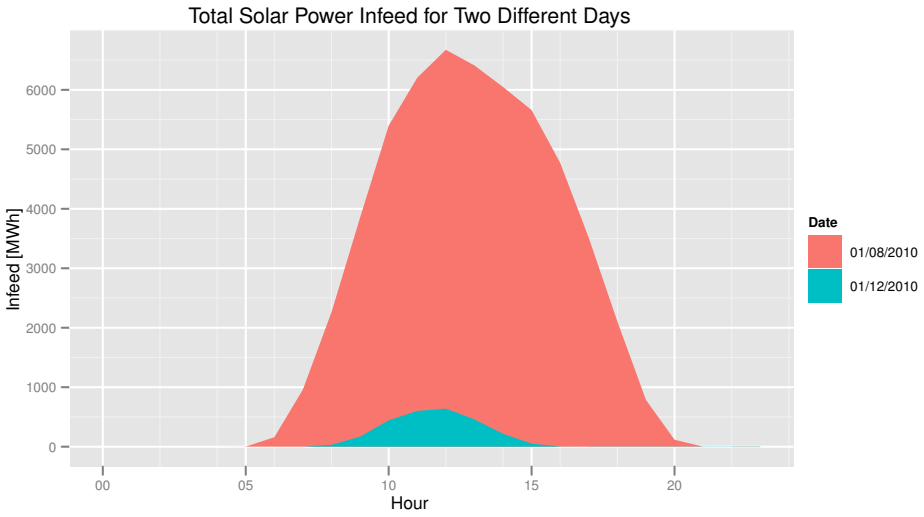

Figure 8: Solar power infeed in Germany for two days in 2010.

and its stationary distribution is $N(0, \frac{\sigma^2}{2\theta})$.

Using the notation from definition 2.3 we say that wind infeed efficiency is modelled as logitnormal.

We assume independence of W_t^{load} and W_t^{wind}, which is equivalent to assuming independence in the evolution of wind infeed and electricity demand. This is sensible, as there is no economic or meteorological reason to assume that wind and demand fluctuations should be correlated.

4 Model for solar power infeed

The daily infeed pattern of solar (intra-day seasonality) is illustrated in figure 8 for a summer and winter day in 2010. The shape of the infeed curve is similar and both days have a certain period of zero infeed. However, length and amount of infeed differs remarkably. Infeed starts earlier and lasts longer on the summer day and it has a much higher peak infeed in comparison to the winter day. Looking at time series of solar power infeed we find that the shape of the curve is similar every day. We plot the August 2010 infeed in figure 9.

This very strong pattern gives rise to a model with a deterministic daily pattern and a stochastic model with daily resolution. We propose to model the daily maximum and deduce the distribution of infeed over the day from historical data. In the following we formalize those ideas.

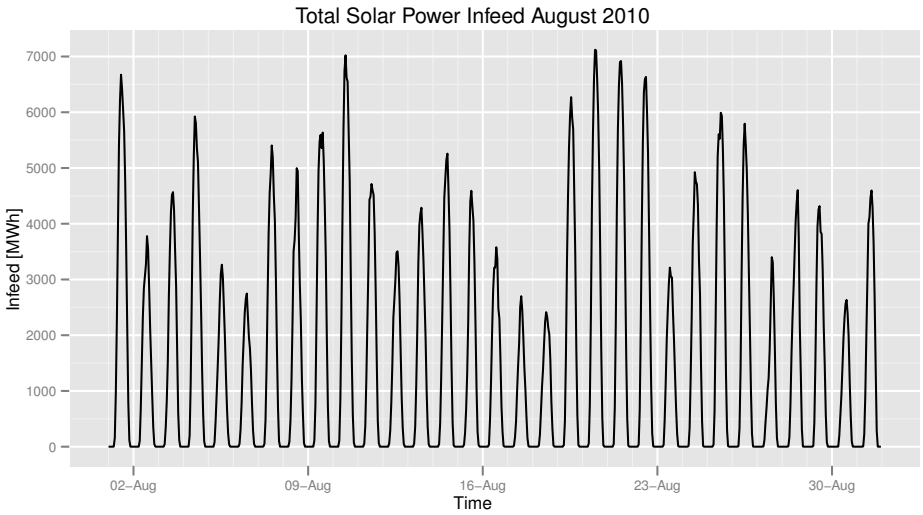

Figure 9: Solar infeed for Germany in August 2010.

Definition 4.1 (Day-count function)**.** The *day-count function*

$$d : [0, T] \to \mathbb{N}_0 \tag{18}$$

is defined by

$$(d_t = n) \equiv (t \text{ is on the n-th day}), \tag{19}$$

starting with 0, i.e. $d_0 = 0$.

In other words, d enumerates the days in $[0, T]$. For each day, we define the daily maximum process $\tilde{M}$.

Definition 4.2 (Daily maximum process)**.** The *daily maximum process* of solar efficiency is defined as

$$\tilde{M}_i^{\text{solar}} = \text{logit}\left(\max_{(t:d_t=i)}\left(E_t^{\text{solar}}\right)\right), i = 0, 1, \ldots, d_T. \tag{20}$$

In figure 10 we plot the daily maximum process for our dataset. Data ranges from 01/08/2010 to 31/07/2011[14]. A 50-day moving average indicates that there is seasonality in the data. Similar to the wind power model,

[14] Actual infeed data is provided by European Energy Exchange AG (2012). For installed capacity we assume 10.644 GW and 17.320 GW for 2010 and 2011, respectively. We use a linear interpolation of installed solar capacity between the beginning and end of our data set. In 2011 there was, especially in the second half of the year, a very strong rise in installed solar capacity, so we use the installed capacity which has been published by European Energy Exchange AG (2012) on 01/07/2011. This year there was a lot of snow covering solar panels in winter (December, January), a very sunny spring (April, May) and a rainy summer (June, July). This year might be considered untypical, but due to a lack of more data we work with this dataset.

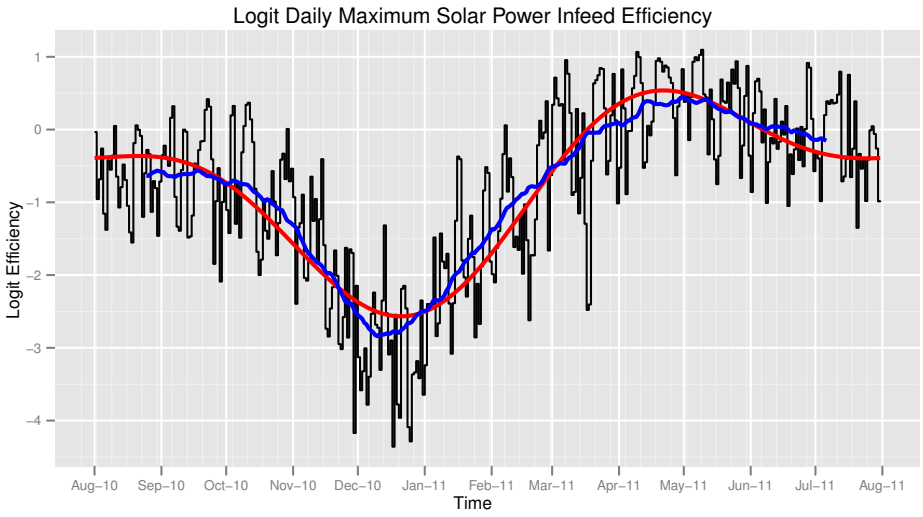

Figure 10: Solar infeed daily maximum process, 50-day moving average (blue) and estimated seasonality (red).

we deseasonalize the daily maximum process using

$$\eta_t^{\text{solar}} = a_1 \cos(2\pi t + b_1) + a_2 \cos(4\pi t + b_2) + c, \tag{21}$$

which is a seasonality able to capture two peaks per year. It fulfills the condition in equ. (12). The moving average and the seasonality estimate are plotted in figure 10. The figure shows that the daily maximum process tends to have similar levels for a few consecutive days. The process is fluctuating around the seasonality, which motivates the choice of a mean-reverting process for the random part. Looking at the process from a time-series point of view we can analyze its partial autocorrelation function. There is strong evidence that an autoregressive model of order one is appropriate. As we have been working with continuous processes throughout this work, we choose an Ornstein-Uhlenbeck process to model the daily maximum.

Model 4.3 (Model for solar efficiency daily maximum)**.** *The model for the* deseasonalized solar efficiency daily maximum $\bar{M}_t^{\text{solar}}$ *is an Ornstein-Uhlenbeck process, i.e.*

$$d\bar{M}_t^{\text{solar}} = -\theta^{\text{solar}} \bar{M}_t^{\text{solar}}\, dt + \sigma^{\text{solar}}\, dW_t^{\text{solar}}, \quad \bar{M}_0^{\text{solar}} = m_0, \tag{22}$$

where

m_0 *is the initial value,*

Statistic	No Transformation	Logit	Deseasonalized Logit
mean	0.358	-0.798	0.000
median	0.364	-0.396	0.026
standard deviation	0.209	0.973	0.703
skewness	0.069	-0.496	-0.262
kurtosis	1.855	1.980	3.140
minimum	0.013	-2.567	-2.470
maximum	0.750	0.538	1.844

Table 2: Statistical figures for the solar power daily maximum efficiency data without transformation and with a logit transformation.

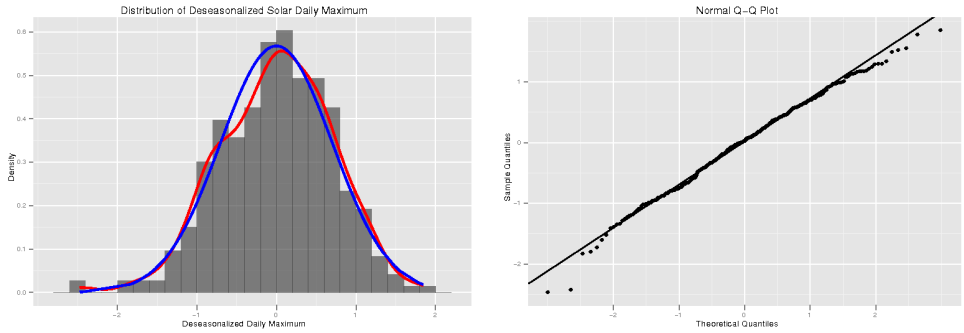

Figure 11: Distribution of deseasonalized daily maximum of solar power infeed efficiency. The left plot includes the histogram, empirical distribution (red line), and a fitted normal distribution (blue line), the right plot is the quantile-quantile plot against the normal distribution.

θ^{solar} *is the mean reversion speed, and*

σ^{solar} *is the volatility.*

As for wind efficiency, we plot a histogram and a quantile-quantile plot of the deseasonalized daily maximum data in figure 11. It shows that the normality assumption, which is implicit in model 4.3, is reasonable. This is also supported by the statistical figures in table 2.

We should point at a little inconsistency in notation. In definition 4.2 we formulated the daily maximum process as a discrete process, but model 4.3 is in continuous time. This will not pose any problems on our work, as in simulations we choose the time-interval to be one day for this process. For the sake of a clean notation, one could define $\bar{M}_i = \max_{(t:d_t=i)} \left(\bar{M}_t^{\text{solar}}\right)$.

For the transformation from the daily maximum to the single hours over the day we use a family of deterministic functions based on historical data. This can be interpreted as the inverse transformation to the daily maximum process (see definition 4.2) and is called *daily pattern transformation.*

Definition 4.4 (Daily pattern transformation)**.** The *daily pattern transformation* is a family of functions

$\{\delta_i, i = 0, \ldots, d_T\}$ with

$$\delta_i : \{t : d_t = i\} \times (0,1) \to [0,1]. \tag{23}$$

A reasonable daily pattern transformation is

$$\delta_i(t,x) = x \sum_{k=1}^{24} c_k \mathbf{1}_{t \in (\text{k-th hour of the day})},\ c_k \in [0,1]\ \forall\ k = 1,2,\ldots,24, \tag{24}$$

which uses a constant proportion of the daily maximum for each hour of the day. We use equ. (24) in the case study in section 6.

Model 4.5 (Model for solar power efficiency)**.** *The model for solar power efficiency E_t^{solar} at time $t \in [0,T]$ is*

$$E_t^{\text{solar}} = \delta_{d_t}\left(t, \text{logit}^{-1}\left(\eta_t^{\text{solar}} + \bar{M}_t^{\text{solar}}\right)\right), \tag{25}$$

where

- *$\bar{M}_t^{\text{solar}}$ is the deseasonalized daily maximum efficiency following model 4.3,*
- *η_t^{solar} is a deterministic seasonality in the daily maximum efficiency, and*
- *δ_{d_t} is the daily pattern transformation for the day d_t.*

As for the wind infeed model, we assume independence between the driving Brownian motions of wind, load, and solar, i.e. W_t^{wind}, W_t^{load}, and, W_t^{solar}, respectively. However, we note that despite the independence of the driving factors, there is some relation in the final models due to the seasonality functions. This is also supported by our empirical analysis, which found no significant correlation between the deseasonalized processes.

5 Residual Demand Model

We combine the approaches for wind and solar power infeed to model residual demand.

Model 5.1 (Model for residual demand)**.** *Suppose a model for total system load L_t, model 3.1 for wind power efficiency E_t^{wind} and model 4.5 for solar power efficiency E_t^{solar}. Assume deterministic functions for installed capacity of wind and solar, IC_t^{wind} and IC_t^{solar}, respectively. The residual demand R_t, i.e. the amount of electricity to be produced by plants other than wind and solar, is modelled as*

$$R_t := L_t - IC_t^{\text{wind}} \cdot E_t^{\text{wind}} - IC_t^{\text{solar}} \cdot E_t^{\text{solar}}. \tag{26}$$

Proposition 5.2. *Suppose model 5.1 with model 1.1 for total system load and assume independence of* W_t^{load}, W_t^{wind}, *and* W_t^{solar}. *Then the distribution of* R_t *is the convolution*

$$\begin{aligned} f_{R_t}(r) = \int_0^1 \int_0^1 & \phi_{\mu^L,\sigma^L}\left(r + IC^{\text{wind}}e + IC^{\text{solar}}\delta_{d_t}(t,m)\right) \cdot \\ & \frac{1}{e(1-e)}\ \phi_{\mu^W,\sigma^W}\left(\text{logit}(e)\right) \cdot \\ & \frac{1}{m(1-m)}\ \phi_{\mu^M,\sigma^M}\left(\text{logit}(m)\right) de\ dm, \end{aligned} \tag{27}$$

where $\phi_{\mu,\sigma}$ *is the normal density with mean* μ *and variance* σ^2, *and*

$$\mu^L = \psi_t + l_0 e^{-\theta^{\text{load}}t}, \tag{28}$$

$$\mu^W = \eta_t^{\text{wind}} + e_0 e^{-\theta^{\text{wind}}t}, \tag{29}$$

$$\mu^M = \eta_t^{\text{solar}} + m_0 e^{-\theta^{\text{solar}}t}, \tag{30}$$

$$\left(\sigma^L\right)^2 = \frac{(\sigma^{\text{load}})^2}{2\theta^{\text{load}}}(1 - e^{-2\theta^{\text{load}}t}), \tag{31}$$

$$\left(\sigma^W\right)^2 = \frac{(\sigma^{\text{wind}})^2}{2\theta^{\text{wind}}}(1 - e^{-2\theta^{\text{wind}}t}), \tag{32}$$

$$\left(\sigma^M\right)^2 = \frac{(\sigma^{\text{solar}})^2}{2\theta^{\text{solar}}}\left(1 - e^{-2\theta^{\text{solar}}t}\right). \tag{33}$$

6 Case Study

We apply the residual demand model to a simple supply/demand model and simulate hourly price paths of the German spot market for the year 2012 based on a calibration using data up to 31/07/2011. The intention of this section is to assess the influence of wind and solar infeed on spot and futures prices. Therefore the spot price model we use is not to be seen as the main contribution of our work. It rather serves as a tool to study the residual demand model in more detail and to demonstrate its effect on modeled prices. In practical applications, one should choose one of the more sophisticated supply side representations, which have been proposed in the literature (see section 1).

Demand-Side

We use model 1.1 for the average total system load prevailing at the peak hours of the day, i.e. between 8 am and 8 pm. This average preserves the weekly pattern and is regular enough to not hide the autocorrelation

within the volatility. The yearly seasonality on business days[15] is assumed

$$y_t := a\cos(2\pi t + b) + c. \tag{34}$$

Demand on non-business days is lower due to less consumption in industry and offices (weekly seasonality). We use a constant proportion of y_t for those days. Therefore the seasonality on a daily scale is

$$\psi_t = (1 - w_1\mathbf{1}_{\{t\in W_1\}} - w_2\mathbf{1}_{\{t\in W_2\}})y_t, \tag{35}$$

where W_1 and W_2 are two disjunct groups of non-business days[16].

For the intra-day seasonality we adopt an idea of Smeers and de Maere (2010) and use a time-dependent intra-day load curve $\delta^L_{d_t}$ transforming the daily average peak demand to the single hours of the day. Using the notation from model 1.1 the load model reads

$$L_t = \delta^L_{d_t}\left(t, \psi_t + l_t\right). \tag{36}$$

Calibration of the Demand Model

We use hourly load data for Germany from 01/08/2010 through 31/07/2011 provided by ENTSOE[17] for the calibration of the load seasonality and process parameters. We do not use a longer time-series, as the economic crisis in 2009 and the beginning of 2010 lead to a downshift in electricity demand, which is not continuing in 2011. We found that the downshift influences the calibration procedure and leads to an underestimated load seasonality.

We calibrate the yearly seasonality y_t on business days using least squares and estimate the non-business day corrections w_1 and w_2 as the mean deviations from the estimated yearly seasonality. For the intra-day load curves δ^L_t we use step-functions with 24 steps different for each month of the year, i.e.

$$\delta^L_t(t,x) = x\sum_{k=1}^{24} c^L_k\mathbf{1}_{t\in(\text{k-th hour of the day})},\ c_k > 0\ \forall\ k = 1,2,\ldots,24. \tag{37}$$

For calibration of c^L_k we calculate the mean value of the ratio between actual load and the daily average peak demand. We show in figure 12 actual load data and our seasonality estimate including the

[15] *Business days* are all days of the year except for weekends and public holidays.

[16] We distinguish between Sundays and public holidays (W_1), and partial holidays (i.e. public holiday in not all German Federal Lands), bridging days (i.e. a Friday/Monday after/before a public holiday), the Christmas week (i.e. 28th to 31st December) and Saturdays (W_2).

[17] `https://www.entsoe.eu`

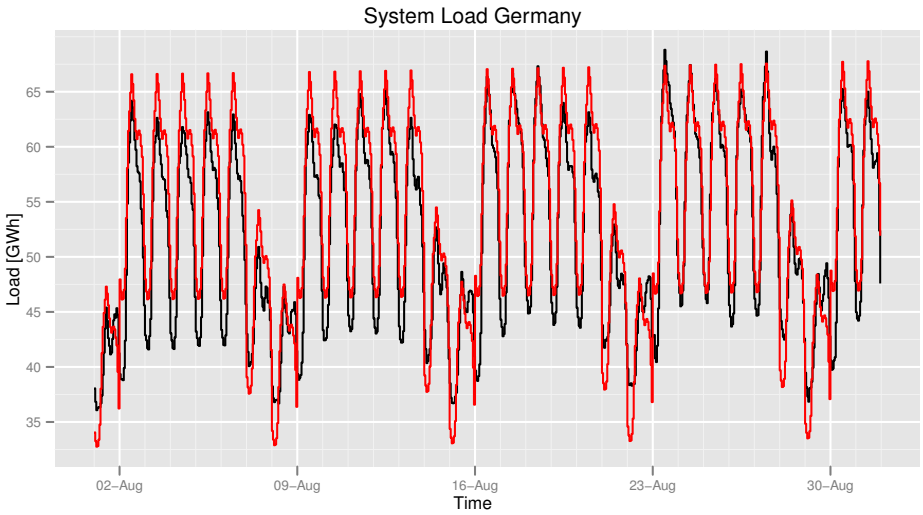

Figure 12: Actual load and seasonality estimate (red) for August 2010.

yearly, weekly and daily model. Finally we calibrate an Ornstein-Uhlenbeck process to the deviations between seasonality estimate and actual load peak average. The estimated parameters are given in table 3.

Calibration of Wind Model

For the calibration of the wind model we use the same data as in section 3. As the efficiency process is stationary this is not inconsistent with the shorter time-series used in load and solar calibration. The estimated parameters are in table 3. We find that the distribution of wind infeed efficiency is unimodal at any time $t > 0$.

Calibration of Solar Model

The solar model is calibrated on the data used in section 4. The estimates are also in table 3 and we find that the distribution of the daily maximum efficiency process is unimodal. For the daily pattern transformation (see definition 4.4) we use the functional form from equ. (24). The calibration is similar to the hourly load shape function. Separately for each month we calculate the mean of

$$\frac{\text{actual infeed for that hour}}{\text{daily maximum infeed}} \tag{38}$$

to determine $c_k, k = 1, \ldots, 24$.

Seasonality		Stochastic Process	
Parameter	Estimate	Parameter	Estimate
Load			
a	4.019	θ^{load}	128.017
b	-0.183	σ^{load}	36.431
c	66.649		
w_1	18.197		
w_2	11.786		
Wind			
a	0.311	θ^{wind}	91.151
b	0.002	σ^{wind}	15.155
c	-1.999		
Solar			
a_1	-1.230	θ^{solar}	261.817
b_1	0.476	σ^{solar}	16.087
a_2	-0.614		
b_2	0.093		
c	-0.798		

Table 3: Calibrated parameters of the residual demand model for Germany.

Technology	Scenario A	Scenario B	Scenario C
wind	29.548	30.769	33.073
solar	19.000	20.510	20.027

Table 4: Estimated installed capacity by technology for the year 2012 in GW based on scenarios from 50hertz et al. (2011) and assuming a constant growth rate for each technology.

Installed Capacity

By construction of our model we need to specify values for installed capacity of wind and solar. We base our estimates on scenarios for installed capacity from 50hertz et al. (2011). We obtain constant growth rates for each scenario and technology and calculate values for installed capacity in 2012 (see table 4). An alternative method to predict installed capacity is to look at power plants under construction and their expected completion date. This is especially suitable for short time horizons and wind power. Solar panels, however, are mounted mainly on private houses and have a very short time-to-build, so data on units planned or under construction can hardly be obtained.

Supply-Side

Motivated by Barlow (2002) we model the supply-side as a deterministic function $f : \mathbb{R} \to \mathbb{R}$ of residual demand, i.e.

$$S_t = f(R_t), \tag{39}$$

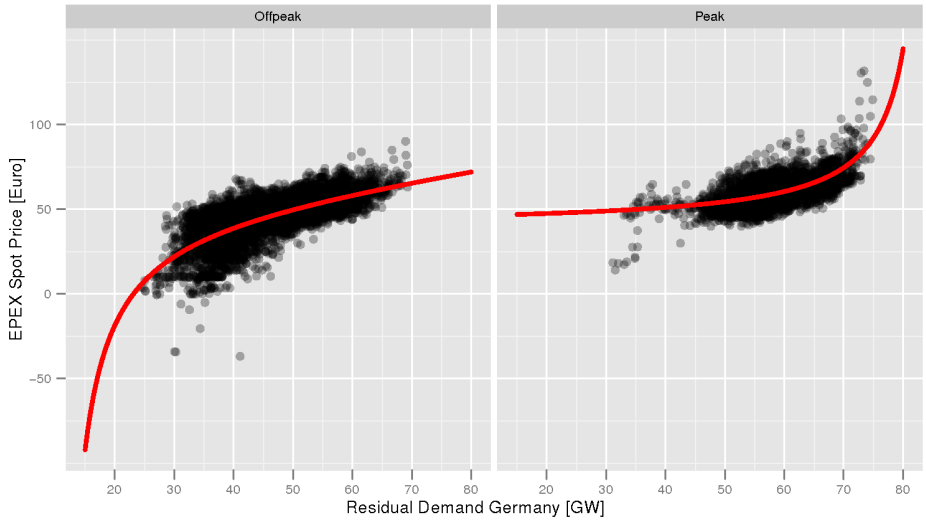

Figure 13: Residual demand against spot price and estimated supply functions (red).

where S_t denotes the spot price of power and R_t residual demand at time t. The desired properties of the function $f(\cdot)$ are motivated by figure 13, which shows historical data[18] on residual demand against spot price. The figure shows a sharp increase in price at a residual demand at about 75 GWh, and on the other hand some negative prices at low residual demand. Between those extremes, the plot suggest a linear relation.

We split the data in peak and offpeak hours, as on the EEX all products are traded for base (this is all hours of the day), peak (weekdays from 8am to 8pm), and offpeak (all but peak) hours, respectively. Therefore such a distinction does enlarge the database which can be used to calibrate the model. Moreover, it simplifies calibration of the supply function. The following functions provide a reasonable fit to the data with only two (three) parameters for peak (offpeak) hours.

Model 6.1 (Supply functions for peak and offpeak)**.** *The supply-function $f : \mathbb{R} \to [p_{floor}, p_{cap}]$ maps residual demand to price. For offpeak hours the supply-function is*

$$f^{offpeak}(x) = \begin{cases} \max\left(p_{floor}, a + \frac{b}{x - x_{floor}} + cx\right) & x > x_{floor} \\ p_{floor} & x \leq x_{floor}. \end{cases} \tag{40}$$

For peak hours it is

$$f^{peak}(x) = \begin{cases} \min\left(p_{cap}, a + \frac{b}{x_{cap} - x}\right) & x < x_{cap} \\ p_{cap} & x \geq x_{cap}. \end{cases} \tag{41}$$

[18] Data ranges from 01/08/2010 to 31/07/2011. We are using this short time frame for calibration, as we have data on solar infeed for this period only.

We found that an additional linear term in the peak supply-function is not significant for the German market. The model parameters for price cap and floor, p_{floor}, p_{cap}, respectively, and load cap and floor, x_{floor}, x_{cap}, respectively, are not calibrated to data but fixed to market-specific values. In case of the German market, the price boundaries set by the exchange are $p_{floor} = -3000$ and $p_{cap} = 3000$. The load boundaries are less obvious, but we found $x_{floor} = 10$ and $x_{cap} = 85$ to be reasonable. The choice is motivated by the fact that 10 GW of online conventional generation seems to be the minimum to ensure system stability[19]. The load cap at 85 GW is justified by guaranteed capacity arguments. According to Bundesministerium für Wirtschaft und Technologie (2011) the guaranteed capacity of Germany in the year 2010 has been 89.9 GW. Taking the nuclear moratorium[20] into account we find that 85 GW of remaining guaranteed capacity is sensible.

Using least-squares, we calibrate model 6.1 on the historical spot price data and residual demand (see figure 13). Therefore all model components are estimated under the historical measure. We also calibrated the supply-function parameters to quoted prices of electricity futures. Using 1000 simulations of the residual demand model under Scenario A (see before) the supply functions are fitted to the quarterly futures from 1st of August 2011 (bold-printed data in table 6). The estimated parameters are in table 5. This calibration procedure can be compared to the concept of existence and calibration under a risk-neutral measure, which is justified by no arbitrage arguments. However, on the one hand as our supply-function is deterministic, risk-neutral *measure* is not the appropriate expression[21]. On the other hand, the concept of a risk-neutral measure is generally questionable in electricity markets (due to the essentially non-storability of electricity), which is amongst others pointed out in Lyle and Elliott (2009): *[...] standard risk neutral pricing arguments, (e.g. cost of carry), are not appropriate in the case of power markets.* They therefore price derivatives under the physical measure, but when derivative prices are available (as it is the case for the EEX market), such a calibration essentially neglects available market information. Therefore we choose the parameters in the futures calibration such that it matches the market as close as possible, but assume that the parameters of our residual demand model do not change (again in risk-neutral pricing language, this corresponds to assuming a zero market price of risk for residual demand). The futures-calibrated supply function reflects expected generation costs, which are mainly driven by fuel prices. As this simple model does not incorporate fuel forward prices, this calibration is a way the model can account for changing fuel prices.

Assuming the supply function parameters fixed, the futures prices can also be used to calibrate a load shift,

[19] For example, the installed nuclear capacity in Germany after the moratorium in 2011 is at about 12 GW, and as nuclear is usually considered a must-run plant, this also supports the choice for x_{floor}.

[20] After the moratorium 8.4 GW of installed nuclear capacity (Bundesnetzagentur, 2011a) have been finally switched off, including roughly 2 GW which were already offline for a couple of years due to technical problems. As nuclear generation is generally considered very reliable, a decrease in guaranteed capacity of 5 GW is a reasonable assumption. This is also supported by Bundesnetzagentur (2011a).

[21] We thank an anonymous referee for pointing this out.

Parameter	Spot Calibration	Futures Calibration
Offpeak		
a	43.000	76.522
b	-713.804	-854.985
c	0.491	0.000
Peak		
a	39.425	24.127
b	528.343	1236.171

Table 5: Parameters for peak and offpeak supply function from a calibration on EPEX day-ahead (=spot) prices from 01/08/2010 to 31/07/2011 (spot calibration) and a calibration on EEX futures prices from 01/08/2011 (futures calibration).

i.e. some constant added to the electricity demand seasonality such that simulated futures prices are close to market prices. This concept is more closely related to the *change of measure* concept[22]. For offpeak and peak we found a positive shift of 5.979 GWand 7.439 GW, respectively. We do not proceed our analysis with this calibration, but rather use the futures-calibrated supply-function.

Results

We simulate 5000 paths of residual demand for the year 2012 in order to assess the proposed model. Using the scenarios and supply functions outlined above we calculate hourly spot prices from residual demand simulations. We start with the trajectorial properties of the model as suggested in Geman and Roncoroni (2006) for a judgment of the quality of an electricity price model. A good trajectorial fit is important for the valuation of path-dependent derivatives. Moreover, many complex risk-management tools require price trajectories as an input.

Figure 14 shows sample price paths of our model. The intra-day and weekly shapes of simulated prices are displayed in figure 15. The observed spot trajectory in figure 3 is less regular, but due to our simple supply side representation this model naturally cannot capture all the risks inherent in the market. However, the occurrence of both positive and negative spikes, as well as their magnitude is nicely reproduced. Moreover the model is able to reproduce the stochastic change of the daily residual load profile depending on the magnitude of renewable infeed during that day, which is illustrated in figure 16. A model only based on load generates the same intraday profile for both days, whereas the residual demand model is able to produce different profiles. Therefore we believe that our model is well suited to generate trajectories with the stylized facts of observed spot prices in recent years.

Using the simulated paths we calculate forward prices. We compare our results to futures price quotes from the EEX from 01/08/2011. However, we note that the simple model set up in this case study is stationary and

[22]The constant can be thought of as a risk-neutral mean-reversion level of the demand process l_t, which is the result from a change of measure assuming that the market-price of (load) risk is independent of the load level.

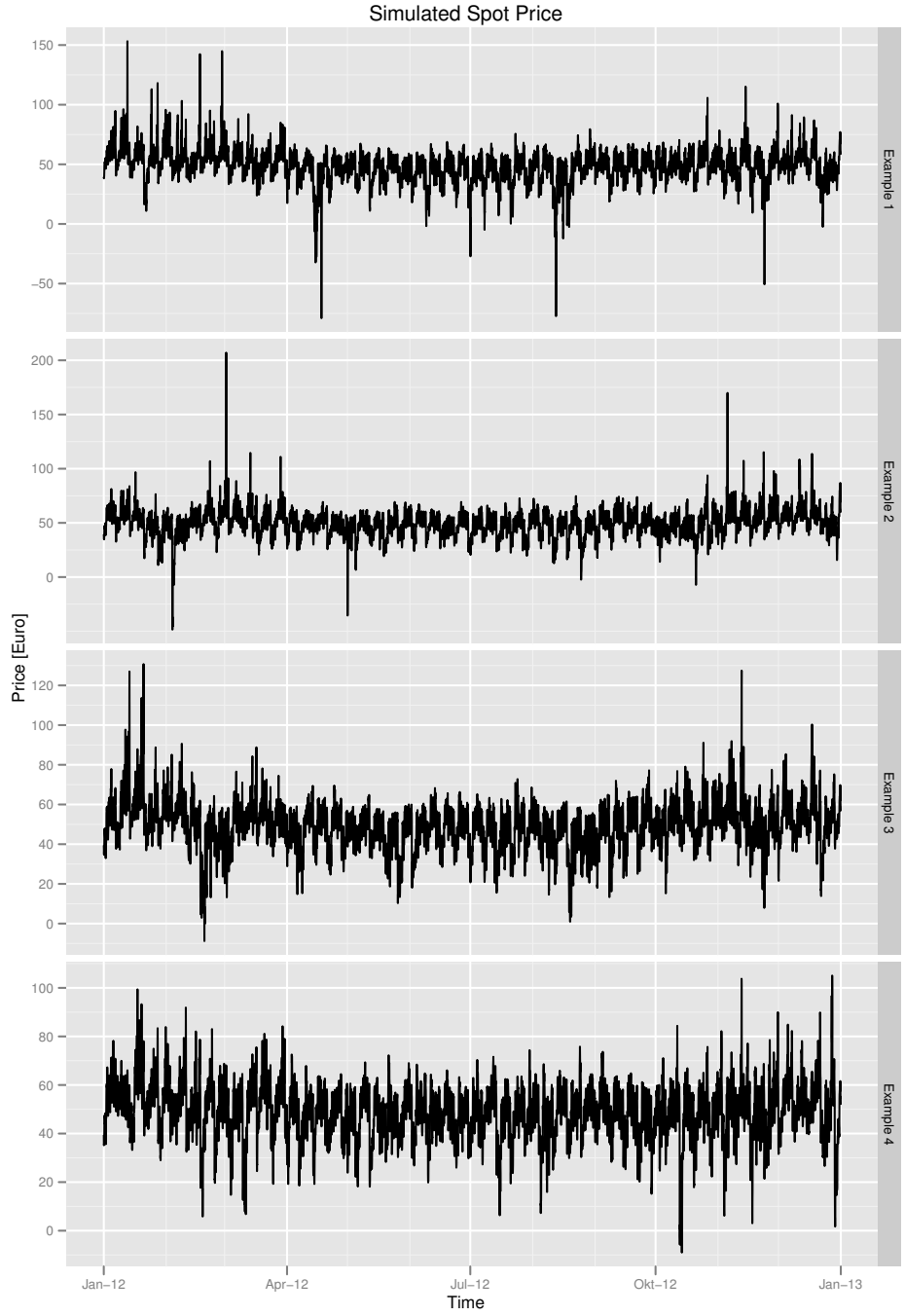

Figure 14: Sample trajectories of hourly simulated spot prices for 2012 under Scenario A.

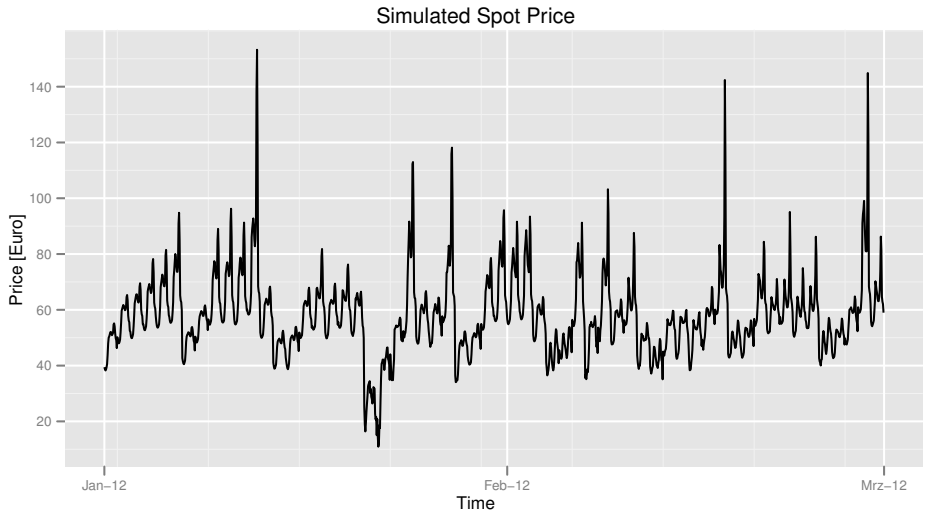

Figure 15: Detail of sample trajectory of hourly simulated spot prices for 2012 under Scenario A.

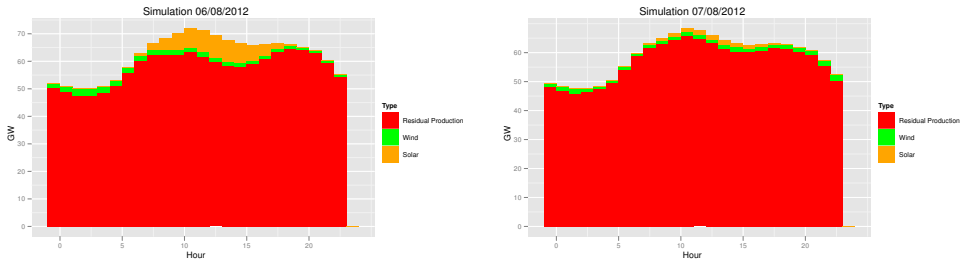

Figure 16: Simulated demand profiles for days with high and low solar infeed, respectively.

therefore in general not well suited for the pricing of derivatives like futures or options. This is also pointed out in Barlow (2002): *Since the price arises from a model for each of the supply and demand curves for power, it is easy in principle to incorporate additional factors to account for long-term effects, or changes in market structure. Such extensions of our model would be essential before it could satisfactorily deal with options and futures prices.* On the other hand the calculation of forward prices can help us to assess the fitting quality of our model with respect to seasonal behavior and show some effects of renewables on market prices. Therefore we continue with a study on futures prices, keeping in mind that the model captures only the risk inherent in load, wind, and solar fluctuations. It does in particular ignore changes in the conventional supply structure like fluctuating fuel and emission prices, power plant outages, and others.

Electricity futures have a delivery period and fulfillment can be instantaneously (which is common for exchange traded products) or at maturity. For instantaneous fulfillment we have the following result.

Proposition 6.2 (Valuation of a forward with instantaneous fulfillment)**.** *The time-t price of a electricity*

	Market	Spot Calibration				**Futures** Calibration			
Product	Price	Price	SD	Forward Premium		Price	SD	Difference	
Base	57.94	49.29	1.04	8.65	(14.93%)	57.95	1.14	-0.01	(-0.02%)
Peak	71.89	59.85	0.57	12.04	(16.75%)	71.91	1.32	-0.02	(-0.03%)
Offpeak	50.21	43.44	1.42	6.77	(13.49%)	50.21	1.33	0.00	(0.00%)
Peak Q1	79.41	63.60	1.49	15.81	(19.90%)	80.70	3.48	-1.29	(-1.62%)
Peak Q2	63.90	56.13	0.64	7.77	(12.15%)	63.22	1.50	0.68	(1.06%)
Peak Q3	64.94	57.38	0.72	7.56	(11.64%)	66.14	1.68	-1.20	(-1.85%)
Peak Q4	79.20	62.22	1.40	16.98	(21.43%)	77.47	3.27	1.73	(2.18%)
Offpeak Q1	53.13	48.17	1.64	4.96	(9.34%)	53.55	1.19	-0.42	(-0.79%)
Offpeak Q2	47.52	39.30	3.66	8.22	(17.30%)	47.20	3.59	0.32	(0.67%)
Offpeak Q3	47.44	40.39	3.36	7.05	(14.85%)	48.04	3.27	-0.60	(-1.26%)
Offpeak Q4	52.76	45.91	2.08	6.85	(12.99%)	52.05	1.70	0.71	(1.35%)

Table 6: Market prices for 2012 futures products (01/08/2011, source `www.eex.de`) and simulation results under Scenario A in EUR/MWh. The absolute standard deviation (SD) and the difference to market price (absolute and as percentage) is given for all simulations. The bold printed products have been used in the futures calibration. The first block are yearly and the second quarterly products, respectively. The remaining months were not yet traded. The difference between simulated and market prices is calculated and also given as percentage relative to market price. In case of spot calibration, this difference is known as *forward premium*.

forward contract with instantaneous fulfillment and delivery period $[T_1, T_2]$ *is*

$$F_t^{\mathbb{Q}}(T_1, T_2) = \frac{r}{e^{r(T_2-T_1)} - 1} \int_{T_1}^{T_2} e^{r(T_2-T)} \mathbb{E}^{\mathbb{Q}}[S_T|\mathcal{F}_t] \, dT, \tag{42}$$

where $\mathbb{Q}$ *is the market measure (i.e. a risk-neutral measure equivalent to the real-world measure* $\mathbb{P}$ *and chosen by the market) and* r *the risk-free interest rate.*

Proof. The forward price (strike price) $K = F_t^{\mathbb{Q}}(T_1, T_2)$ is chosen such that the contract has zero expected value at time t:

$$0 = \mathbb{E}^{\mathbb{Q}} \left[\int_{T_1}^{T_2} e^{r(T_2-T)} (S_T - K) \, dT|\mathcal{F}_t \right]. \tag{43}$$

The payoff $S_T - K$ is received at time T (instantaneous fulfillment) and reinvested (or borrowed, depending on the sign of $S_T - K$) at the risk-free rate r until the final settlement at T_2. Solving equ. (43) for K proves the assertion. □

We assume a risk-free rate of 2% in all our calculations. In table 6 we compare futures prices under Scenario A for the spot and futures calibration, i.e. we calculate $F_t^{\mathbb{P}}(T_1, T_2)$ and $F_t^{\mathbb{Q}}(T_1, T_2)$, respectively. The forward premium[23] is found positive for all products ranging from 11% to 21% of market price. The premium is the

[23] The forward premium is defined as $F_t^{\mathbb{Q}}(T_1, T_2) - F_t^{\mathbb{P}}(T_1, T_2)$, i.e. the difference between the forward price evaluated under the risk-neutral measure (which is the observed market price) and the real-world measure. There is extensive research on the forward premium in electricity markets, cf. Bessembinder and Lemmon (2002), Longstaff and Wang (2004), Benth and Meyer-Brandis (2009), and Biegler-König et al. (2011).

highest for the products *Peak Q1* and *Peak Q4* (first and fourth quarter 2012). This supports the assumption that the nuclear moratorium added uncertainty in the market, especially the risk of positive spikes in times of high demand (winter months). The futures calibration is able to significantly reduce the deviations between simulated and market prices. The missing baseload supply shifts demand in the winter months to the steep region of the supply curve. This can also be seen in the price spread between the *Peak Q1/Q4* and *Peak Q2/Q3*[24]. Historcally, this has been at about 6 EUR. Our historical calibration is mainly based on data from before the moratorium, so it produces the *pre-moratorium* spread of about 6 EUR. However, the *post-moratorium* spread turns out to be at about 14 EUR, which the model can reproduce unter the futures calibration. This argument supports the model, as it can incorporate structural changes on the supply side despite of its simple representation. In general, the offpeak results are closer to observed prices as the peak products. This has been expected as the offpeak supply-function has three parameters, whereas for the peak supply-function only two parameters were used to calibrate. Generally, the good representation of the seasonality in prices also supports the model.

The standard deviations differ remarkably between the analyzed products and show seasonal behavior. In general, a higher standard deviation is expected when demand during the delivery period is within areas of high gradient of the supply functions. Looking at the quarterly contracts, we find that for the peak products there is a lower standard deviation in the second and third quarter compared to others, whereas for the offpeak products the situation is vice versa. In order to assess this in more detail, we show boxplots for simulated monthly futures prices 2012 in figure 17. The box, which contains 50% of the simulations, is small compared to the absolute size of the price. There are outliers for both offpeak and peak simulations. For the offpeak products, all outliers are below the box, meaning that in these paths the average price for the corresponding month is below the mean. For the peak futures, there are much less outliers, but the variance structure is significantly different between different periods. The winter months with high demand show the biggest variation in prices. The spring and summer months with very high solar infeed show a much smaller price range. This is due to the peak shaving effect, which reduces the spike risk in this period. The lowest prices (incl. outliers) are observed for April and May, which have the highest solar seasonality, but also many public holidays are on weekdays in those months[25]. A similar behavior can be observed for December due to the reduced demand during the Christmas week.

The analysis conducted above was based on Scenario A. As we have deterministic installed capacities in our model we can use the same paths to study prices under a different scenario. We work with the spot-calibrated supply functions in the following and we compare the simulated prices in table 7. We find that the prices under

[24] We thank an anonymous referee for pointing us torwards this point.
[25] The EEX peak futures deliver every weekday independent of public holidays.

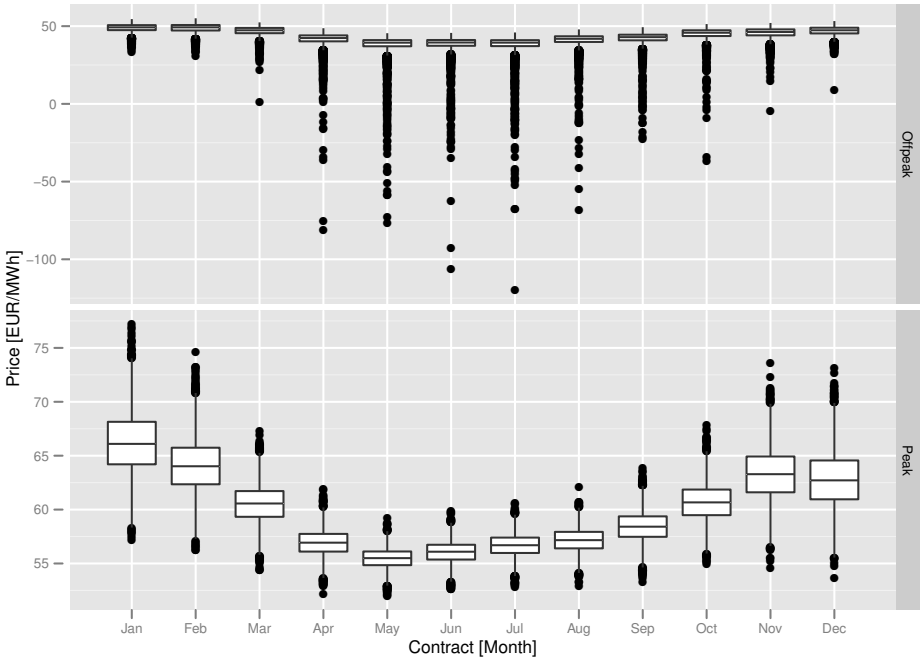

Figure 17: Boxplots of simulated prices for the monthly futures 2012 based on the spot calibration and Scenario A.

Scenario B are lower compared to Scenario A, and Scenario C shows even lower prices than Scenario B. The decrease in price is due to the greater installed capacities for wind and solar in Scenario B and C compared to Scenario A, which, by construction, reduces wholesale electricity prices. The picture is less clear when looking at the volatility (standard deviation) in the market. We consider the quarterly contracts. Volatility increases for all offpeak contracts, because higher renewable infeed brings residual demand more often in the steep region of the supply function. For the peak contracts, however, volatility does not change significantly, expect for the *Peak Q2* product (which is the quarter with the on average highest solar infeed). We conclude that increased capacity of renewables decreases wholesale electricity market prices (*merit-order effect*), but increases volatility in times of low demand. In order to separate the effects of wind and solar we analyse the model's sensitivity with respect to wind and solar installed capacity separately. We base our analysis on the spot calibration and Scenario A and add one GW of installed capacity of wind (Scenario *SensWind*) and solar (Scenario *SensSolar*), respectively. The results are also displayed in table 7. Considering the *Base* contract we find that the overall price effect of wind is stronger than of solar. In peak hours the effect is balanced. In the sunny quarters *Q2* and *Q3* solar has also considerable effect on the offpeak prices[26]. In the most expensive products (*Peak Q1* and *Peak Q4*), solar shows less price decrease compared to wind. For the

[26] Remember that offpeak includes the whole weekend and also, in summer, part of the sunshine falls in the offpeak hours before 8am and after 8pm (see also figure 8).

Product	A (reference)		B (difference)		C (difference)		SensWind (difference)		SensSolar (difference)	
	Price	SD	Price	SD	Price	SD	Price	SD	Price	SD
Base	48.79	1.04	- 0.50	0.22	- 1.19	0.65	- 0.27	0.14	- 0.11	0.02
Peak	59.85	0.57	- 0.32	0.00	- 0.52	0.01	- 0.11	0.00	- 0.12	0.00
Offpeak	43.44	1.42	- 0.60	0.37	- 1.56	1.04	- 0.36	0.23	- 0.10	0.04
Peak Q1	63.60	1.49	- 0.37	0.00	- 0.69	0.03	- 0.17	0.01	- 0.12	- 0.01
Peak Q2	56.13	0.64	- 0.34	- 0.01	- 0.40	0.02	- 0.06	0.01	- 0.17	- 0.01
Peak Q3	57.38	0.72	- 0.30	0.00	- 0.40	0.02	- 0.07	0.01	- 0.14	- 0.01
Peak Q4	62.22	1.40	- 0.28	0.01	- 0.58	0.03	- 0.15	0.01	- 0.06	- 0.01
Offpeak Q1	48.17	1.64	- 0.39	0.25	- 1.02	0.79	- 0.25	0.15	- 0.05	0.02
Offpeak Q2	39.30	3.66	- 0.86	1.07	- 2.07	2.90	- 0.44	0.62	- 0.19	0.15
Offpeak Q3	40.39	3.36	- 0.74	0.98	- 1.90	2.69	- 0.42	0.62	- 0.13	0.11
Offpeak Q4	45.91	2.08	- 0.42	0.34	- 1.24	1.14	- 0.31	0.26	- 0.02	0.01

Table 7: Simulated futures prices and empirical standard deviation (SD) under different scenarios. Scenario A is the reference scenario, for all other cases the differences with respect to the corresponding value of Scenario A are given. For Scenario A, B, and C, respectively, see table 4. Scenario *SensWind* and *SensSolar* are the results for a sensitivity analysis with respect to 1 GW increase in installed capacity of wind and solar, respectively.

offpeak products, additional wind capacity generally leads to a stronger decrease in price as for additional solar capacity. Given the already high share of installed solar capacity the results indicate that new solar capacity does not have a higher merit-order effect than wind. Moreover, the sensitivity analysis supports our assumptions on price volatility. In times of low demand both wind and solar add volatility to the market, whereas volatility can be reduced in peak hours with high demand.

7 Conclusions

We proposed an extension to electricity demand models for markets with a considerable infeed from wind and solar power plants. It can be applied to existing supply/demand models to account for infeed from those renewables. As we model renewable infeed as demand reduction, our model is suitable for markets with a guaranteed infeed and feed-in tariff for production from renewables (like Germany). If there is no such system, production from renewables will bid at price zero (i.e. their marginal production costs) on the exchange. In this case, our approach is only suitable when additionally assuming that no negative prices are allowed at the exchange. The wind and solar infeed models can also be used in applications other than electricity pricing, e.g. in the optimization of power plant portfolios, power plant dispatching or economic models.

Due to the separation of total demand, wind infeed, and solar infeed a calibration of the model is straightfor-

ward, as data for each component is separately available. Moreover, using our model one can utilize existing supply/demand models to evaluate the impact of wind and solar infeed on electricity prices. The concept of not including installed capacity in the model (i.e. as trend) is motivated by the fact that the development of renewables can hardly be deduced from time series of historical data, as it is much more driven by exogenous factors, especially political decisions. When there is much uncertainty in the development of installed capacity, one could evaluate the model for different scenarios, possibly weighted by their expected probability of occurrence (those scenarios can be evaluated in a single simulation). The recent development of the German installed solar capacity proves that this *political risk* needs to be considered. This can also be used in risk-management or investment departments of energy utilities to assess their risk-exposure w.r.t. different development schemes.

As we have no requirements on the model for total system load utilities can continue using their existing model for system load and extend it using our wind and solar infeed model to a more accurate residual demand model. In ongoing research, we apply the more sophisticated supply/demand model of Aïd et al. (2009) on the German market using the Residual Demand Model proposed in this paper for the demand side.

References

50hertz, Amprion, EnBW Transportnetze AG, and TenneT TSO (2011). Szenariorahmen für den Netzentwicklungsplan 2012.

Aïd, R., L. Campi, A. N. Huu, and N. Touzi (2009). A structural risk-neutral model of electricity prices. *International Journal of Theoretical and Applied Finance 12*(07), 925–947.

Aïd, R., L. Campi, and N. Langrené (2012, February). A Structural Risk-Neutral Model for Pricing and Hedging Power Derivatives. *Mathematical Finance* (to appear).

Aksoy, H. (2004). Stochastic generation of hourly mean wind speed data. *Renewable Energy 29*(14), 2111–2131.

Barlow, M. (2002). A diffusion model for electricity prices. *Mathematical Finance 12*, 287–298.

Benth, F. E. and T. Meyer-Brandis (2009). The information premium for non-storable commodities. *Journal of Energy Markets 2*(3).

Bessembinder, H. and M. L. Lemmon (2002). Equilibrium Pricing and Optimal Hedging in Electricity Forward Markets. *Finance 17*(3).

Biegler-König, R., F. E. Benth, and R. Kiesel (2011). An Empirical Study on the Information Premium in Electricity Markets.

Bundesministerium für Umwelt Naturschutz und Reaktorsicherheit (2010). Erneuerbare Energien in Zahlen 2010.

Bundesministerium für Umwelt Naturschutz und Reaktorsicherheit (2012). Erneuerbare Energien in Zahlen 2012.

Bundesministerium für Wirtschaft und Technologie (2011). Monitoring-Bericht zur Versorgungssicherheit.

Bundesnetzagentur (2011a). Auswirkungen des Kernkraftwerk-Moratoriums auf die Übertragungsnetze und die Versorgungssicherheit.

Bundesnetzagentur (2011b). Monitoringbericht 2011.

Burger, M., B. Klar, A. Müller, and G. Schindlmayr (2004). A spot market model for pricing derivatives in electricity markets. *Quantitative Finance 4*(1), 109–122.

Carmona, R. and M. Coulon (2012). A survey of commodity markets and structural models for electricity prices. In *Proceedings from the special thematic year at the Wolfgang Pauli Institute, Vienna,*.

Carmona, R., M. Coulon, and D. Schwarz (2011). Electricity price modeling and asset valuation: a multi-fuel structural approach.

Carta, J. A., P. Ramirez, and S. Velazquez (2008). Influence of the level of fit of a density probability function to wind-speed data on the WECS mean power output estimation. *Energy Conversion and Management 49*(10), 2647–2655.

Carta, J. A., P. Ramirez, and S. Velazquez (2009). A review of wind speed probability distributions used in wind energy analysis. *Renewable and Sustainable Energy Reviews 13*(5), 933–955.

Cartea, A. and P. Villaplana (2008, December). Spot price modeling and the valuation of electricity forward contracts: The role of demand and capacity. *Journal of Banking & Finance 32*(12), 2502–2519.

Coulon, M. and S. Howison (2009). Stochastic Behaviour of the Electricity Bid Stack: from Fundamental Drivers to Power Prices. *The Journal of Energy Markets 2*(1), 29–69.

European Energy Exchange AG (2012). Transparency in Energy Markets.

Fahrmeir, L. and G. Tutz (2001). *Multivariate Statistical Modelling Based on Generalized Linear Models* (2nd ed.). Springer Series in Statistics. Springer.

Frederic, P. and F. Lad (2008). Two Moments of the Logitnormal Distribution. *Communications in Statistics - Simulation and Computation 37*(7), 1263–1269.

Geman, H. and A. Roncoroni (2006). Understanding the Fine Structure of Electricity Prices. *The Journal of Business 79*(3), 1225–1261.

Johnson, N. L. (1949). Systems of Frequency Curves Generated by Methods of Translation. *Biometrika 36*(1), 149–176.

Longstaff, F. A. and A. W. Wang (2004). Electricity Forward Prices: A High-Frequency Empirical Analysis. *The Journal of Finance 59*(4), 1877–1900.

Lyle, M. R. and R. J. Elliott (2009). A simple hybrid model for power derivatives. *Energy Economics 31*(5), 757–767.

Mead, R. (1965). A Generalised Logit-Normal Distribution. *Biometrics 21*(3), 721–732.

Pirrong, C. and M. Jermakyan (2008, December). The price of power: The valuation of power and weather derivatives. *Journal of Banking & Finance 32*(12), 2520–2529.

Renewable Energy Policy Network for the 21st Century (2011). Renewables 2011 - Global Status Report.

Smeers, Y. and G. de Maere (2010). The valuation of power futures based on optimal dispatch. *The Journal of Energy Markets 3*(3), 27–50.